Human Molecular Genetics, 2018, Vol. 27, No. 16 2805–2816

doi: 10.1093/hmg/ddy189
Advance Access Publication Date: 16 May 2018
Original Article

ORIGINAL ARTICLE

Loss of fragile X protein FMRP impairs homeostatic synaptic downscaling through tumor suppressor p53 and ubiquitin E3 ligase Nedd4-2

Kwan Young Lee[1], Kathryn A. Jewett[1], Hee Jung Chung[1,2] and Nien-Pei Tsai[1,2,*]

[1]Department of Molecular and Integrative Physiology, School of Molecular and Cellular Biology and [2]Neuroscience Program, University of Illinois at Urbana-Champaign, Urbana, IL 61801, USA

*Correspondence to be addressed at: 407 South Goodwin Avenue, Urbana, IL 61801, USA. Tel: +1 2172445620; Fax: +1 217331133; Email: nptsai@illinois.edu

Abstract

Synaptic scaling allows neurons to homeostatically readjust synaptic strength upon chronic neural activity perturbations. Although altered synaptic scaling has been implicated to underlie imbalanced brain excitability in neurological disorders such as autism spectrum disorders and epilepsy, the molecular dysregulation and restoration of synaptic scaling in those diseases have not been demonstrated. Here, we showed that the homeostatic synaptic downscaling is absent in the hippocampal neurons of *Fmr1* KO mice, the mouse model of the most common inherited autism, fragile X syndrome (FXS). We found that the impaired homeostatic synaptic downscaling in *Fmr1* KO neurons is caused by loss-of-function dephosphorylation of an epilepsy-associated ubiquitin E3 ligase, neural precursor cell expressed developmentally down-regulated gene 4-2, Nedd4-2. Such dephosphorylation of Nedd4-2 is surprisingly caused by abnormally stable tumor suppressor p53 and subsequently destabilized kinase Akt. Dephosphorylated Nedd4-2 fails to elicit 14-3-3-dependent ubiquitination and down-regulation of the GluA1 subunit of AMPA receptor, and therefore impairs synaptic downscaling. Most importantly, using a pharmacological inhibitor of p53, Nedd4-2 phosphorylation, GluA1 ubiquitination and synaptic downscaling are all restored in *Fmr1* KO neurons. Together, our results discover a novel cellular mechanism underlying synaptic downscaling, and demonstrate the dysregulation and successful restoration of this mechanism in the FXS mouse model.

Introduction

Homeostatic scaling describes a feedback modulation whereby chronic activity perturbation is rebalanced through the readjustment of synaptic strength or intrinsic excitability to maintain network stability (1,2). This scaling allows a circuit to accurately determine the baseline for long-term plasticity events and also maintains a physiological range of excitability (3). Impaired scaling has been implicated to underlie imbalanced neuronal excitability in many neurological disorders (4); however, whether and how homeostatic scaling is dysregulated in those diseases remains unclear.

Fragile X syndrome (FXS) is the most common form of inherited autism and cognitive impairment, caused by transcriptional silencing or loss-of-function mutations in the *Fmr1* gene, which encodes the fragile X mental retardation protein (FMRP). FXS patients and the mouse model of FXS, the *Fmr1* knock-out (KO), both show elevated neuronal excitability (5–7). This hyperexcitability is often associated with or triggered by neuronal

Received: March 6, 2018. **Revised:** May 7, 2018. **Accepted:** May 9, 2018

activity stimulation, suggesting a potential dysregulation in the homeostatic control of neuronal excitability. However, this area has not been closely examined. One mechanism underlying homeostatic control of neuronal excitability operates through modulation of ion channel stability by ubiquitination (8). One promising ubiquitin (Ub) E3 ligase that often targets ion channels is neural precursor cell expressed developmentally down-regulated gene 4-like, Nedd4-2. Nedd4-2 belongs to the Nedd4 family of Ub E3 ligases (9) and is encoded by an epilepsy-associated gene (10). Nedd4-2 has been shown to regulate neuronal excitability (11,12). However, it remains unknown whether Nedd4-2 is involved in homeostatic synaptic scaling and how its function may be dysregulated in FXS.

In this study, we uncovered a surprising connection between loss of FMRP, tumor suppressor p53 and Nedd4-2 in synaptic downscaling after activity stimulation and revealed how they are molecularly dysregulated in *Fmr1* KO neurons. Most importantly, we were able to restore the downscaling mechanism by pharmacologically inhibiting p53 in *Fmr1* KO neurons. These results reveal a novel cellular mechanism underlying synaptic scaling and provide a new perspective for understanding the imbalance of brain circuit excitability observed in FXS and autism spectrum disorders (ASDs).

Results

Homeostatic synaptic downscaling is absent in Fmr1 KO hippocampal neurons

Because the loss of FMRP leads to neuronal hyperexcitability in FXS, we aimed to determine whether homeostatic synaptic downscaling is depending on FMRP. We employed a widely used method for induction of homeostatic synaptic downscaling, the application of GABA(A) receptor antagonist picrotoxin (PTX) (100 μM for 48 h) in dissociated mouse primary hippocampal neuron cultures, and observed a reduction in amplitude, but not frequency (Fig. 1A; Supplementary Material, Table S1), of miniature excitatory postsynaptic currents (mEPSCs) in wild-type (WT) hippocampal neurons. These observations indicate a successful induction of homeostatic synaptic downscaling in WT neurons. When we performed the same experiments using *Fmr1* KO mouse hippocampal neurons to assess the requirement of FMRP in downscaling, we found that while mEPSC amplitude is basally elevated in *Fmr1* KO neurons when compared with WT neurons as previously observed (13), PTX treatment failed to reduce mEPSC amplitude in *Fmr1* KO neurons (Fig. 1B; Supplementary Material, Table S1). These data indicate FMRP is required for synaptic downscaling after PTX treatment.

Down-regulation of total and surface excitatory glutamate α-amino-3-hydroxy-5-methyl-4-isoxazolepropionic acid receptors (AMPARs) is one of the major mechanisms underlying synaptic downscaling (14,15). To determine whether such phenomenon is impaired in *Fmr1* KO, we performed confocal imaging on dissociated hippocampal neurons treated with PTX or dimethyl sulfoxide (DMSO, as a vehicle, 0.1%) for 48 h. As expected, WT neurons exhibited significant reductions in total and surface levels of both GluA1 and GluA2 after PTX treatment (Fig. 1C). However, none of these effects were apparent in *Fmr1* KO neurons (Fig. 1D), supporting our hypothesis that FMRP is required for chronic activity-induced down-regulation of AMPAR.

To determine if the lack of homeostatic downscaling in the *Fmr1* KO cultures was from insufficient activity stimulation by PTX, we employed a multi-electrode array recording system to record extracellular spontaneous spikes in primary cortical neuron cultures made from WT or *Fmr1* KO mice. As shown in Supplementary Material, Figure S1, both WT and *Fmr1* KO cultures exhibited similar elevation of spontaneous spikes and burst activity after PTX treatment for 30 min. Together, our data suggest that *Fmr1* KO cultures successfully respond to PTX but fail to elicit homeostatic synaptic downscaling.

Nedd4-2-, but not Nedd4-1-, mediated GluA1 ubiquitination is impaired in Fmr1 KO neurons

Down-regulation of AMPAR during synaptic downscaling can be mediated by ubiquitination (11,14–16). To test whether AMPAR ubiquitination is altered in *Fmr1* KO, we performed immunoprecipitation (IP) of GluA1 or GluA2 from cortical neuron cultures treated with PTX or DMSO for 48 h, followed by western blotting with anti-Ub antibody to detect ubiquitinated GluA1 or GluA2. We focused on GluA1 and GluA2 subunits because they have been shown to participate in synaptic scaling (17–19). We used antibodies against their N-termini to avoid potential interference with ubiquitination; when GluA1 and GluA2 are ubiquitinated it primarily occurs at their C-termini (16). Using cortical neuron cultures enables us to obtain a sufficient amount of protein samples for biochemical experiments. As shown in Figure 2A, elevated ubiquitination of both GluA1 and GluA2 in WT neurons after PTX treatment was observed. However, such ubiquitination was not observed in *Fmr1* KO neurons. We also performed IP of Ub followed by western blotting for GluA1 or GluA2 in cultures treated with PTX or DMSO for 48 h to validate our observation and obtained very similar results (Supplementary Material, Fig. S2). Because the difference between WT and *Fmr1* KO is more significant with GluA1 than GluA2, and GluA1 ubiquitination mediates the levels of surface AMPAR (14,15), we hypothesized that impaired GluA1 ubiquitination leads to the absence of homeostatic downscaling in *Fmr1* KO neurons.

GluA1 ubiquitination can be mediated by neural precursor cell expressed developmentally down-regulated protein 4 (Nedd4-1) and neural precursor cell expressed developmentally downregulated gene 4-like (Nedd4-2), two Ub E3 ligases that belong to the same protein family (9). To study whether Nedd4-1 and Nedd4-2 exhibit differential activity toward GluA1 ubiquitination in WT versus *Fmr1* KO neurons during homeostatic downscaling, we partially purified Nedd4-1 and Nedd4-2 using IP from WT or *Fmr1* KO cortical neuron cultures treated with PTX or DMSO for 48 h. We subsequently used precipitated Nedd4-1 or Nedd4-2 to pull down recombinant GluA1. As shown in Figure 2B, Nedd4-1 from WT and *Fmr1* KO cultures exhibited similar binding affinity toward GluA1 under either PTX or DMSO treatments. Interestingly, while Nedd4-2 from WT cultures showed elevated interaction with GluA1 after PTX treatment, such interaction was reduced when Nedd4-2 is obtained from *Fmr1* KO cultures (the purity of recombinant GluA1 was shown in Fig. 2B3). This phenomenon was also observed when we performed co-IP to measure the interaction between endogenous Nedd4-2 and GluA1 (Supplementary Material, Fig. S3). Because altered interaction between Nedd4-2 and GluA1 was not observed when using immunoprecipitated GluA1 from WT or *Fmr1* KO cultures to pull down recombinant Nedd4-2 (Fig. 2C), we conclude that the reduced interaction between Nedd4-2 and GluA1 in *Fmr1* KO neurons results from altered molecular properties of Nedd4-2. This conclusion is further validated when we use immunoprecipitated Nedd4-2 from WT or *Fmr1* KO cortical neuron cultures

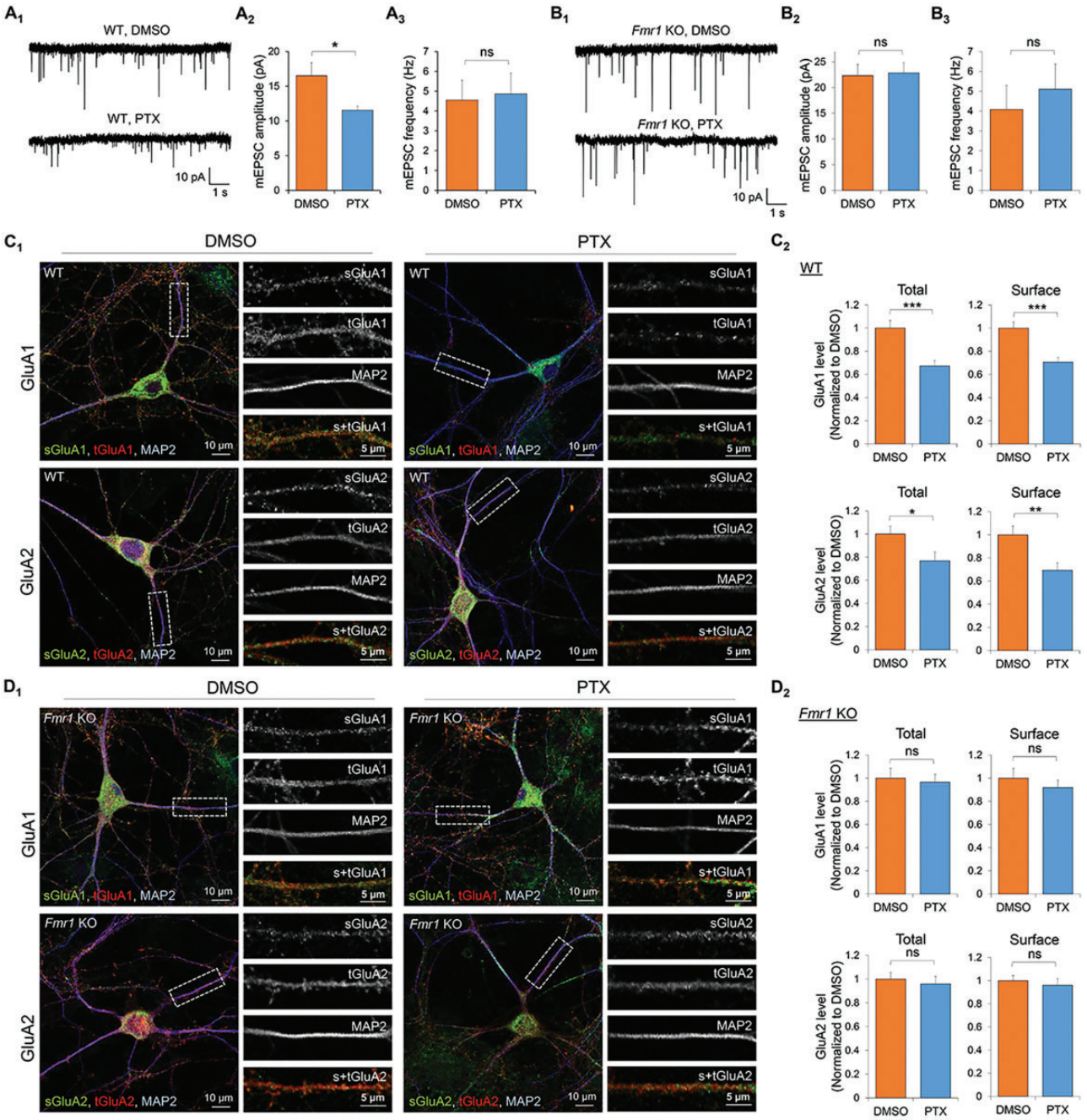

Figure 1. FMRP is required for homeostatic synaptic downscaling. Patch-clamp recording from WT (**A**) or *Fmr1* KO (**B**) mouse hippocampal neurons treated with vehicle (DMSO) or PTX for 48 h. Representative mEPSC traces and quantification of mEPSC amplitude and frequency are shown ($n = 16$–18 for WT and *Fmr1* KO neurons). Immunocytochemistry showing total (t) and surface (s) GluA1 and GluA2 from WT (**C**) or *Fmr1* KO (**D**) hippocampal neurons treated with DMSO or PTX for 48 h. Magnified images of dendrites are shown to the right of the composite image. Quantification on the right ($n = 20$ cells for WT and *Fmr1* KO neurons). Data were analyzed by Student's *t*-test and represented as mean ± SEM with $^{*}P < 0.05$, $^{**}P < 0.01$, $^{***}P < 0.001$, and ns: non-significant.

treated with PTX to perform *in vitro* ubiquitination with recombinant GluA1. As shown in Figure 2D, while Nedd4-1 from WT and *Fmr1* KO cortical neuron cultures exhibits strong yet similar activity toward ubiquitinating GluA1, Nedd4-2 from *Fmr1* KO showed significantly lower activity toward ubiquitinating GluA1. We therefore conclude that the reduced ubiquitination and down-regulation of GluA1 during synaptic downscaling in *Fmr1* KO neurons is likely the result of reduced interaction between Nedd4-2 and GluA1.

Nedd4-2 undergoes dephosphorylation in Fmr1 KO during the induction of downscaling

We have previously demonstrated that the interaction between Nedd4-2 and GluA1 requires an adaptor protein 14-3-3 (12). To determine how 14-3-3 is involved in decreased GluA1 ubiquitination in *Fmr1* KO, we performed co-IP to evaluate the interaction between Nedd4-2 and 14-3-3. As shown, the interaction between Nedd4-2 and 14-3-3 in WT neurons treated with PTX

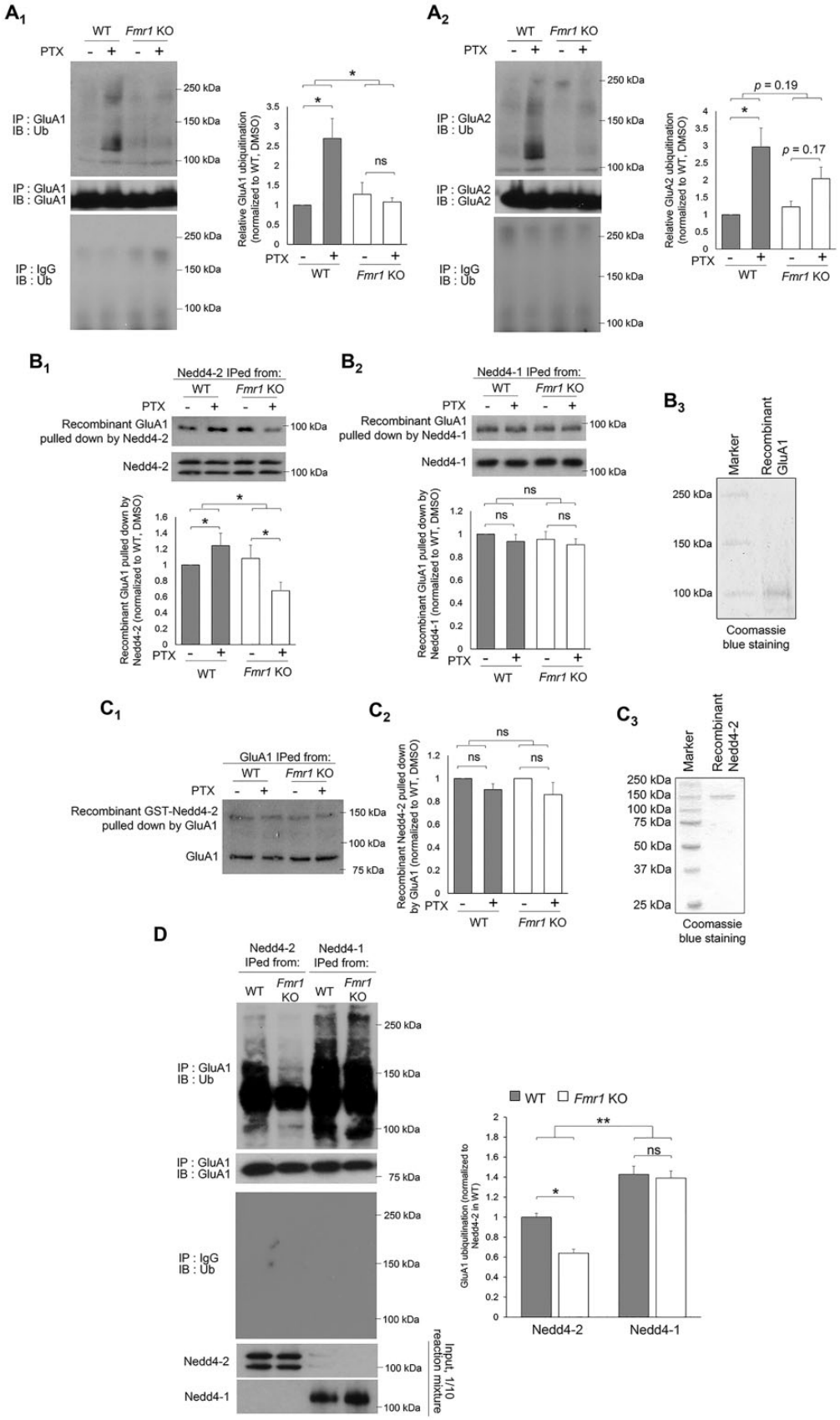

Figure 2. Nedd4-2-mediated GluA1 ubiquitination during homeostatic synaptic downscaling is impaired in *Fmr1* KO neurons. (**A**) Western blots of Ub after IP using anti-GluA1 (A_1) or GluA2 (A_2) antibody from WT or *Fmr1* KO cortical neuron cultures treated with vehicle (DMSO) or PTX for 48 h ($n = 4$). (**B**) Western blots of recombinant GluA1 pulled down by Nedd4-2 (B_1) or Nedd4-1 (B_2) immunoprecipitated from WT or *Fmr1* KO cortical neuron cultures treated with DMSO or PTX for 48 h ($n = 5$ for B_1 and $n = 3$ for B_2). Coomasie blue staining showing the purity of recombinant GluA1 is on the right (B_3). The two distinct bands in Nedd4-2 blots represent two major

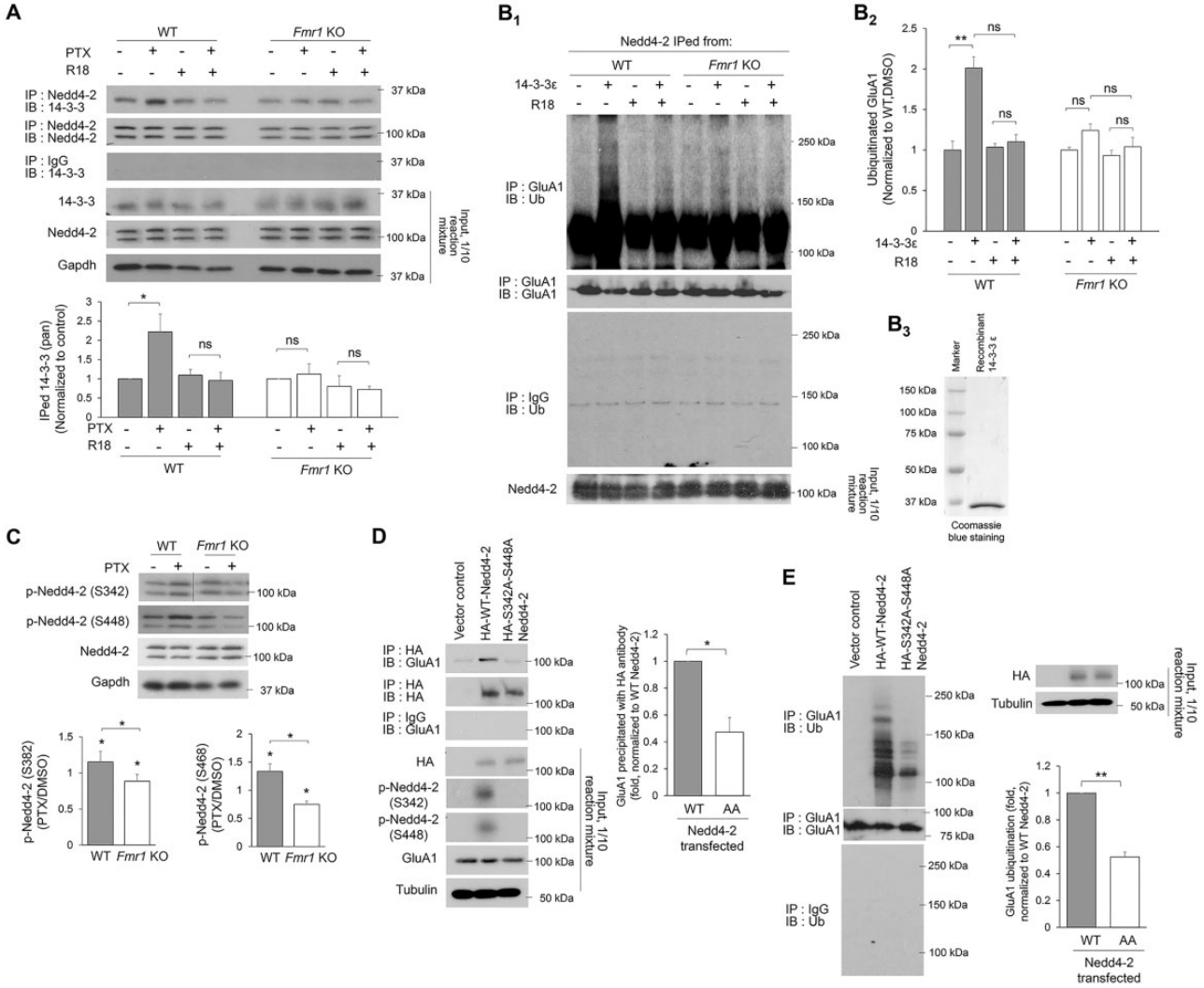

Figure 3. Loss-of-function dephosphorylation of Nedd4–2 disrupts GluA1 ubiquitination in *Fmr1* KO neurons. (**A**) Western blots of 14-3-3 after co-IP of Nedd4-2 using lysates from WT or *Fmr1* KO cortical neuron cultures treated with vehicle (DMSO) or 14-3-3 inhibitor (R18) (0.025 mg/ml) for 1 h following vehicle (DMSO) or PTX treatment for 48 h (two-way ANOVA with Tukey's test, $n = 4$). (**B**) Western blots of Ub or GluA1 after IP with anti-GluA1 antibody following *in vitro* ubiquitination with recombinant GluA1 and Nedd4-2 immunoprecipitated from WT or *Fmr1* KO cortical neuron cultures treated with PTX for 48 h. An addition of recombinant 14-3-3ε or R18 was applied prior to the ubiquitination reaction as labeled in the figure (Two-way ANOVA with Tukey's test, $n = 4$). Coomasie blue staining showing the purity of recombinant 14-3-3ε is on the right (B_3). (**C**) Western blots of phospho-Nedd4-2-S342 and phospho-Nedd4-2-S448 from WT or *Fmr1* KO cortical neuron cultures treated with DMSO or PTX for 48 h (one-sample *t*-test for each genotype and Student's *t*-test for comparison between genotypes, $n = 4$). (**D**) Western blots of GluA1 after co-IP of HA-Nedd4-2 using lysates from HEK cells transfected with GluA1 and control vector, HA-WT-Nedd4-2 or HA-S342A-S448A-Nedd4-2 for 2 days. The intensity of precipitated GluA1 from all samples was normalized to HA-WT-Nedd4-2-transfected cultures (Student's *t*-test, $n = 4$). (**E**) Western blots of Ub after IP using anti-GluA1 antibody and lysates from HEK cells transfected with GluA1 and control vector, HA-WT-Nedd4-2 or HA-S342A-S448A-Nedd4-2 for 2 days Student's *t*-test, $n = 3$). Data are represented as mean ± SEM with $^{*}P < 0.05$, $^{**}P < 0.01$, $^{***}P < 0.001$ and ns: non-significant.

for 48 h was strongly elevated (Fig. 3A). The elevated interaction can be blocked by treatment with a general 14-3-3 inhibitor R18 (0.025 mg/ml) for 1 h prior to co-IP, confirming the specificity of interaction between Nedd4-2 and functional 14-3-3. However, the interaction between Nedd4-2 and 14-3-3 in *Fmr1* KO neurons was not enhanced after PTX treatment (Fig. 3A). To determine how these results are reflected in GluA1 ubiquitination, we performed *in vitro* GluA1 ubiquitination using recombinant GluA1 and immunoprecipitated Nedd4-2 from either WT or *Fmr1* KO cultures treated with PTX for 48 h. GluA1 ubiquitination by Nedd4-2 from WT cultures is enhanced by the addition of recombinant 14-3-3ε, one of the 14-3-3 isoforms known to interact

isoforms of Nedd4-2 as previously reported (12). (**C**) Western blots of recombinant Nedd4-2 (top) pulled down by GluA1 (bottom) immunoprecipitated from WT or *Fmr1* KO cortical neuron cultures treated with DMSO or PTX for 48 h. The difference between WT and *Fmr1* KO cultures was analyzed after normalizing PTX-treated groups to DMSO-treated groups ($n = 4$). Coomasie blue staining showing the purity of recombinant Nedd4-2 is on the right (C_3). (**D**) Western blots of Ub or GluA1 after IP with anti-GluA1 antibody following *in vitro* ubiquitination with recombinant GluA1 and Nedd4-2 or Nedd4-1 immunoprecipitated from WT or *Fmr1* KO cortical neuron cultures treated with PTX for 48 h ($n = 4$). For all experiments, data were analyzed by two-way ANOVA with Tukey's test and represented as mean ± SEM with $^{*}P < 0.05$, $^{**}P < 0.01$ and ns: non-significant.

with Nedd4-2 (12), and such enhancement can be inhibited by R18 (Fig. 3B). As expected, GluA1 ubiquitination was not elevated by the addition of 14-3-3ε when using Nedd4-2 obtained from *Fmr1* KO cultures. These data support our hypothesis that the impaired GluA1 ubiquitination after PTX treatment in *Fmr1* KO neurons results from reduced interaction between Nedd4-2 and GluA1.

The interaction between Nedd4-2 and 14-3-3 can be enhanced when Nedd4-2 is phosphorylated at two of its serine residues, S342 and S448 (20). We found that Nedd4-2 phosphorylation at both residues is elevated in WT cortical neuron cultures after PTX treatment for 48 h (Fig. 3C). Unexpectedly, both residues were significantly dephosphorylated by PTX treatment in *Fmr1* KO cultures (Fig. 3C). To determine whether dephosphorylated Nedd4-2 leads to reduced GluA1 ubiquitination, we co-transfected human embryonic kidney cells with GluA1 and WT- or de-phospho-mimetic Nedd4-2 (S342A-S448A-Nedd4-2) and found that de-phospho-mimetic Nedd4-2 exhibits significantly lower activity toward binding and ubiquitinating GluA1 (Fig. 3D and E). These data suggest a possibility that dephosphorylation of Nedd4-2 after PTX treatment in *Fmr1* KO neurons likely contributes to impaired GluA1 ubiquitination. One interesting observation is that, despite higher phosphorylation of Nedd4-2 under basal conditions in *Fmr1* KO neurons (Fig. 3C), GluA1 does not exhibit elevated ubiquitination when compared with that in WT neurons (Fig. 2A). We suspect that other compensatory mechanisms are reducing the Nedd4-2–GluA1 interaction to counteract hyperactive Nedd4-2 during basal conditions (see more details in the 'Discussion' section).

Loss-of-function dephosphorylation of Nedd4-2 disrupts GluA1 ubiquitination and synaptic downscaling in Fmr1 KO

To determine whether and how Nedd4-2 dephosphorylation contributes to impaired homeostatic synaptic downscaling in *Fmr1* KO neurons, we lentivirally expressed control GFP and human influenza hemagglutinin (HA)-tagged WT- or phosphomimetic Nedd4-2 (S342D-S448D-Nedd4-2) in *Fmr1* KO cortical neuron cultures. We employed phospho-mimetic Nedd4-2 only in *Fmr1* KO neurons because Nedd4-2 is already hyperphosphorylated in WT neurons during downscaling and because our goal was to restore synaptic downscaling in *Fmr1* KO neurons. As shown in Figure 4A, while GluA1 ubiquitination was unaffected by control GFP as expected, it was surprising that expressing HA-WT-Nedd4-2 was sufficient to restore GluA1 ubiquitination after PTX treatment. We reason that such effect is elicited by a portion of HA-WT-Nedd4-2 that remains phosphorylated in *Fmr1* KO neurons upon PTX treatment (Supplementary Material, Fig. S4), and this is likely sufficient to trigger GluA1 ubiquitination. Importantly, in cultures expressing HA-S342D-S448D-Nedd4-2, GluA1 ubiquitination is basally elevated but further effect after PTX treatment is occluded, which is potentially owing to a limit of GluA1 ubiquitination that can be facilitated in healthy cells. When examining surface AMPAR using *Fmr1* KO hippocampal neurons, we observed similar effects; HA-WT-Nedd4-2 expression reduced surface GluA1 after PTX treatment, while HA-S342D-S448D-Nedd4-2 reduced surface GluA1 basally but occluded further reduction after PTX treatment (Fig. 4B). Because the total GluA1 levels in HA-S342D-S448D-Nedd4-2-expressing cultures did not decrease before PTX treatment, our results suggest that GluA1 ubiquitination is sufficient for reducing surface levels of GluA1, but chronic neural activity stimulation is required to initiate GluA1 degradation. These data also suggest that other mechanisms triggered by PTX, and deficient in *Fmr1* KO, are likely required to promote degradation of ubiquitinated GluA1. In regards to GluA2, we did not observe any significant effects in *Fmr1* KO hippocampal neuron cultures expressing either WT- or S342D-S448D-Nedd4-2 (Fig. 4C), consistent with our previous results that GluA2 is not a substrate of Nedd4-2 (11).

When we performed mEPSC recordings to examine homeostatic downscaling, HA-WT-Nedd4-2 restored the reduction of mEPSC amplitude after PTX treatment, while HA-S342D-S448D-Nedd4-2 reduced mEPSC amplitude basally but occluded further reduction after PTX treatment (Fig. 4D; Supplementary Material, Table S1), consistent with the results of surface GluA1 (Fig. 4B). Taken together, we conclude that Nedd4-2 phosphorylation is crucial to reducing synaptic strength through ubiquitination of GluA1 and rectifying Nedd4-2 phosphorylation in *Fmr1* KO neurons after PTX treatment will likely restore homeostatic synaptic downscaling.

Inhibition of p53 restores Nedd4-2 phosphorylation, Nedd4-2-dependent GluA1 ubiquitination and homeostatic synaptic downscaling in Fmr1 KO

Our previous work showed that chronic neural activity elevation activates protein kinase B, also known as Akt, and subsequently leads to murine double minute-2 (Mdm2) phosphorylation and Mdm2-dependent p53 down-regulation (11). Since Nedd4-2 phosphorylation at S342 and S448 residues can be mediated by Akt (20–22), we measured the signaling of Akt and Mdm2-p53 in *Fmr1* KO cortical neuron cultures. As shown in Figure 5A, Mdm2 is basally phosphorylated in *Fmr1* KO neurons, in line with our previous report (23), and PTX treatment failed to further elevate Mdm2 phosphorylation or trigger p53 down-regulation. Although phosphorylated Mdm2 is expected to down-regulate p53 (24,25), the level of p53 in *Fmr1* KO neurons is comparable to that in WT neurons, suggesting a compensatory mechanism is maintaining p53 level or other molecules are interfering with Mdm2-dependent p53 degradation in *Fmr1* KO (see more details in the 'Discussion' section). Most surprisingly, we found that Akt was significantly down-regulated after PTX treatment in *Fmr1* KO neurons, which may explain the dephosphorylation of Nedd4-2 in *Fmr1* KO neurons (Fig. 3C). Because constitutive activity of p53 can lead to destabilization and down-regulation of Akt (26), we tested whether using a p53 inhibitor pifithrin-α (1 μM) can restore Akt levels after PTX treatment in *Fmr1* KO neurons. As shown in Figure 5A, while pifithrin-α alone did not exert an effect on the basal levels of Akt, it restored Akt levels and reduced Nedd4-2 dephosphorylation when employed in combination with PTX in *Fmr1* KO neurons. Most importantly, it restored PTX-induced GluA1 ubiquitination in *Fmr1* KO neurons without significant effects on WT neurons (Fig. 5B; Supplementary Material, Fig. S5). Together, our findings identified a novel signaling pathway underlying abnormal Nedd4-2 dephosphorylation upon chronic neural activity elevation in *Fmr1* KO neurons which can be restored by pharmacologically inhibiting p53.

To determine whether homeostatic synaptic downscaling in *Fmr1* KO neurons can also be restored by the short-term inhibition of p53, we applied pifithrin-α to *Fmr1* KO hippocampal neuron cultures and measured synaptic downscaling. We found that while PTX or pifithrin-α alone did not show an effect on *Fmr1* KO neurons, similar to what we observed in the Akt-Mdm2

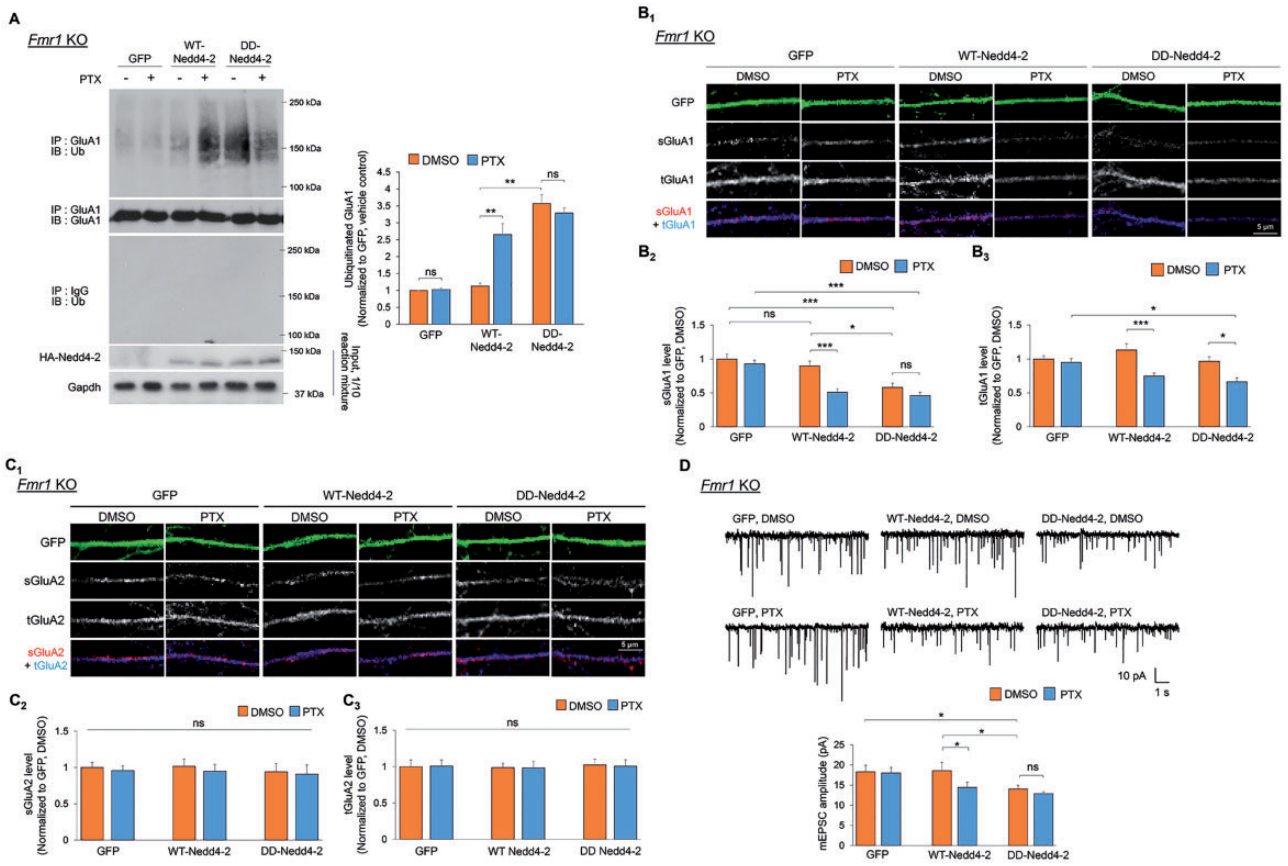

Figure 4. Phosphorylation of Nedd4-2 reduces GluA1 levels and excitatory synaptic strength in *Fmr1* KO neurons. (**A**) Western blots of Ub after IP using anti-GluA1 antibody from *Fmr1* KO cortical neuron cultures lentivirally transfected with control GFP, HA-WT-Nedd4-2 (WT-Nedd4-2), or HA-S342D-S448D-Nedd4-2 (DD-Nedd4-2) and treated with vehicle (DMSO) or PTX for 48 h ($n = 5$). (**B**, **C**) Immunocytochemistry showing total (t) and surface (s) GluA1 and GluA2 in representative dendrites of *Fmr1* KO hippocampal neurons transiently transfected with control GFP, WT-Nedd4-2 or DD-Nedd4-2 and treated with DMSO or PTX for 48 h. Quantification of total or surface GluA1 and GluA2 normalized to the average intensity of that in GFP-transfected, DMSO-treated neurons are on the bottom ($n = 18$–26 cells for *Fmr1* KO neurons). (**D**) Patch-clamp recording from *Fmr1* KO hippocampal neurons transiently transfected with control GFP, WT-Nedd4-2 or DD-Nedd4-2 and treated with DMSO or PTX for 48 h. Representative mEPSC traces and quantification of mEPSC amplitude are shown ($n = 18$–20 for *Fmr1* KO neurons). Data were analyzed by two-way ANOVA with Tukey's test and represented as mean ± SEM with $^{*}P < 0.05$, $^{**}P < 0.01$, $^{***}P < 0.001$ and ns: non-significant.

signaling pathway and GluA1 ubiquitination (Fig. 5), administration of pifithrin-α and PTX together restores synaptic downscaling in *Fmr1* KO neurons, as demonstrated by reduced total and surface GluA1 (Fig. 6A), and by reduced mEPSC amplitude (Fig. 6B; Supplementary Material, Table S1). GluA2 again remains unaffected (Fig. 6C). To validate that our observation with the use of pifithrin-α is specific to p53 and to provide a secondary method to confirm the role of p53 in impaired synaptic downscaling in *Fmr1* KO neurons, we transiently transfected a validated shRNA against p53 (11) or a previously tested non-target shRNA (13,23) in dissociated *Fmr1* KO hippocampal neurons followed by the treatment of PTX or DMSO for 48 h. As shown in Figure 6D and Supplementary Material, Table S1, the cells receiving p53 shRNA, but not non-target shRNA, exhibited homeostatic synaptic downscaling 48 h after PTX treatment. Together, our results demonstrate a restoration of Akt and Nedd4-2 signaling, as well as homeostatic synaptic downscaling in *Fmr1* KO neurons by inhibition of p53.

Discussion

In this study, we present evidence that Nedd4-2-mediated GluA1 ubiquitination and homeostatic synaptic downscaling are absent after chronic activity stimulation by PTX in *Fmr1* KO neurons. Mechanistically, we found that abnormally stable p53 in *Fmr1* KO neurons during induced synaptic downscaling leads to loss-of-function dephosphorylation of Nedd4-2, and subsequently impairs GluA1 ubiquitination (Fig. 7). When using the p53 inhibitor pifithrin-α to mimic inactivation of p53 during synaptic downscaling in WT neurons, GluA1 ubiquitination and synaptic downscaling are restored in *Fmr1* KO neurons. This study demonstrates a novel mechanism by which FMRP mediates synaptic downscaling by maintaining Nedd4-2 phosphorylation and permitting GluA1 ubiquitination during chronic neural activity stimulation. Interestingly, although GluA2 is similarly affected in *Fmr1* KO neurons (Fig. 2A) and is also known to participate in synaptic scaling (27,28), pifithrin-α is able to restore synaptic downscaling in *Fmr1* KO neurons without any significant effect on total or surface GluA2 (Fig. 6C), suggesting the dominant role of GluA1 in impaired synaptic scaling in *Fmr1* KO. It is commonly accepted that homeostatic scaling is bi-directional but it is unknown whether Nedd4-2 is inversely regulated during upscaling and whether Nedd4-2 is also dysregulated during an induction of upscaling in *Fmr1* KO neurons (19). While this current study focuses on the downscaling mechanism based on the prediction that impaired downscaling could contribute to neuronal hyperexcitability (29), which is a profound phenotype in FXS, it would be of particular interest to

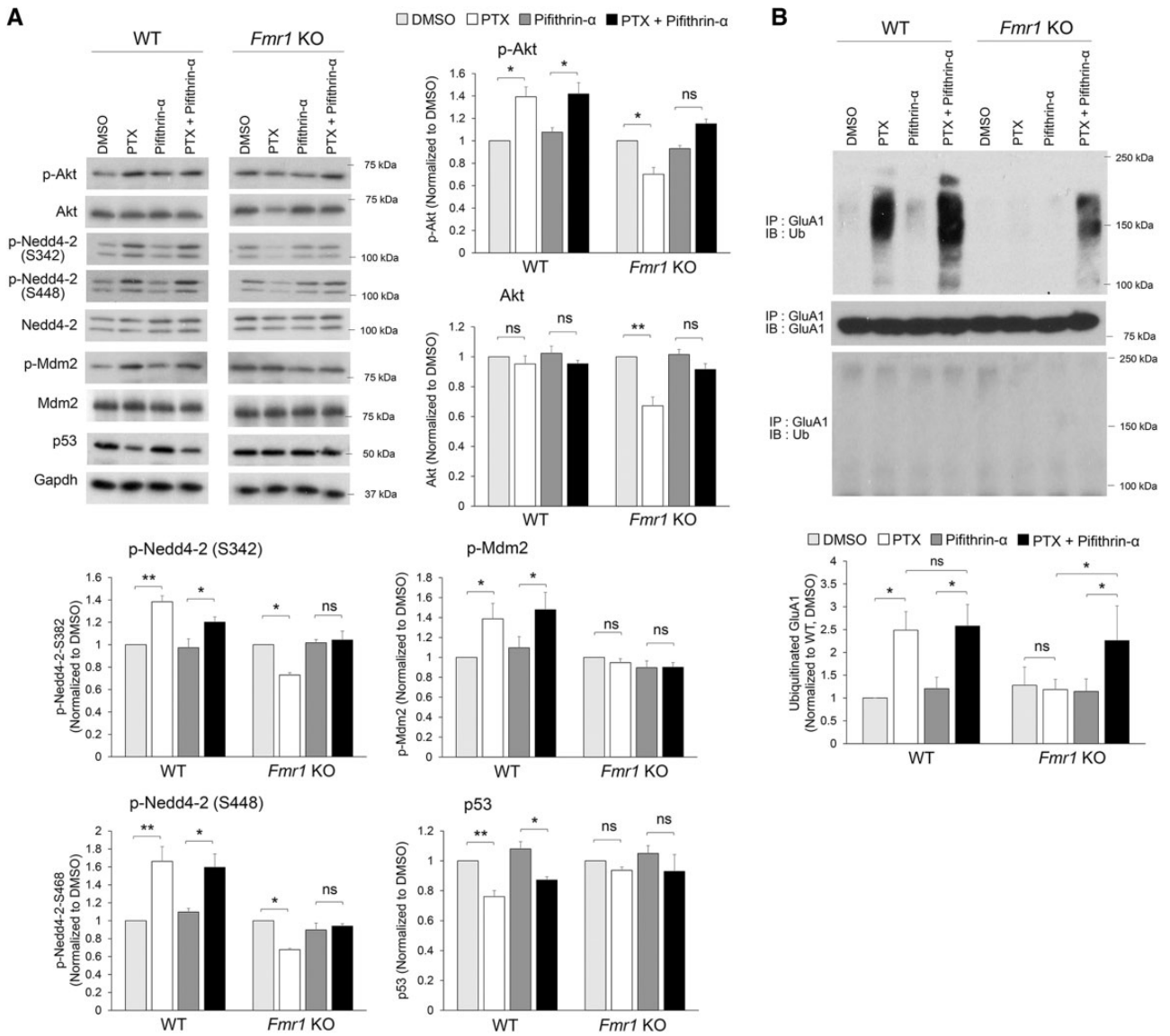

Figure 5. Inhibition of p53 prevents Nedd4-2 dephosphorylation and restores GluA1 ubiquitination in *Fmr1* KO neurons. (**A**) Western blots (left) and quantification (right) of phospho-Akt-S473, total Akt, phospho-Nedd4-2-S342, phospho-Nedd4-2-S448, total Nedd4-2, phospho-Mdm2-S163, total Mdm2, p53 and internal control Gapdh from WT or *Fmr1* KO cortical neuron cultures treated with vehicle (DMSO), PTX, pifithrin-α, or PTX + pifithrin-α for 48 h ($n = 3$–5 independent cultures). (**B**) Western blots of Ub after IP using anti-GluA1 antibody from WT or *Fmr1* KO cortical neuron cultures treated with DMSO, PTX, pifithrin-α or PTX + pifithrin-α for 48 h ($n = 4$). Data were analyzed by two-way ANOVA with Tukey's test and represented as mean ± SEM with $^*P < 0.05$, $^{**}P < 0.01$ and ns: non-significant.

determine whether and how Nedd4-2 and GluA1 ubiquitination are modulated upon chronic activity blockade.

Nedd4-2 and another Nedd4 family member, Nedd4-1, are each an E3 ligase for GluA1. Our data showed that the interaction between Nedd4-2 and GluA1 can be enhanced upon chronic neural activity stimulation, while the interaction between Nedd4-1 and GluA1 appears to be independent of chronic activity stimulation. These results suggest that although both Nedd4-1 and Nedd4-2 are involved in homeostasis of synaptic strength, Nedd4-1 may exert constitutive functions toward GluA1 ubiquitination while Nedd4-2 contributes mainly upon chronic activity stimulation. Our data also suggest that activity-induced GluA1 ubiquitination by Nedd4-2 is mediated by phosphorylation of Nedd4-2 at the S342 and S448 residues. Nedd4-2 can be phosphorylated directly by Akt (22) or indirectly by Akt's downstream pathways, such as mechanistic targeting of rapamycin (mTOR) and serum- and glucocorticoid-inducible kinase 1 (20,21). Akt is reported to be basally active in *Fmr1* KO neurons (30). However, we did not observe enhanced GluA1 ubiquitination or Nedd4-2–GluA1 interaction during basal conditions (Fig. 2A and B). This could be owing to a compensatory effect to reduce Nedd4-2–GluA1 interaction during circuit development, as previously described in *Fmr1* KO mice (31,32). This is also likely true for Mdm2-p53 signaling, in which Mdm2 is basally phosphorylated in *Fmr1* KO neurons (23) but synaptic downscaling is not facilitated accordingly. These observations again emphasize the complexity of FXS. If our predictions are true, it would suggest that a common compensatory mechanism for protein ubiquitination and degradation in *Fmr1* KO may exist. Quantitative measurement of protein ubiquitination and deubiquitination in *Fmr1* KO could test this possibility and is an important future research direction.

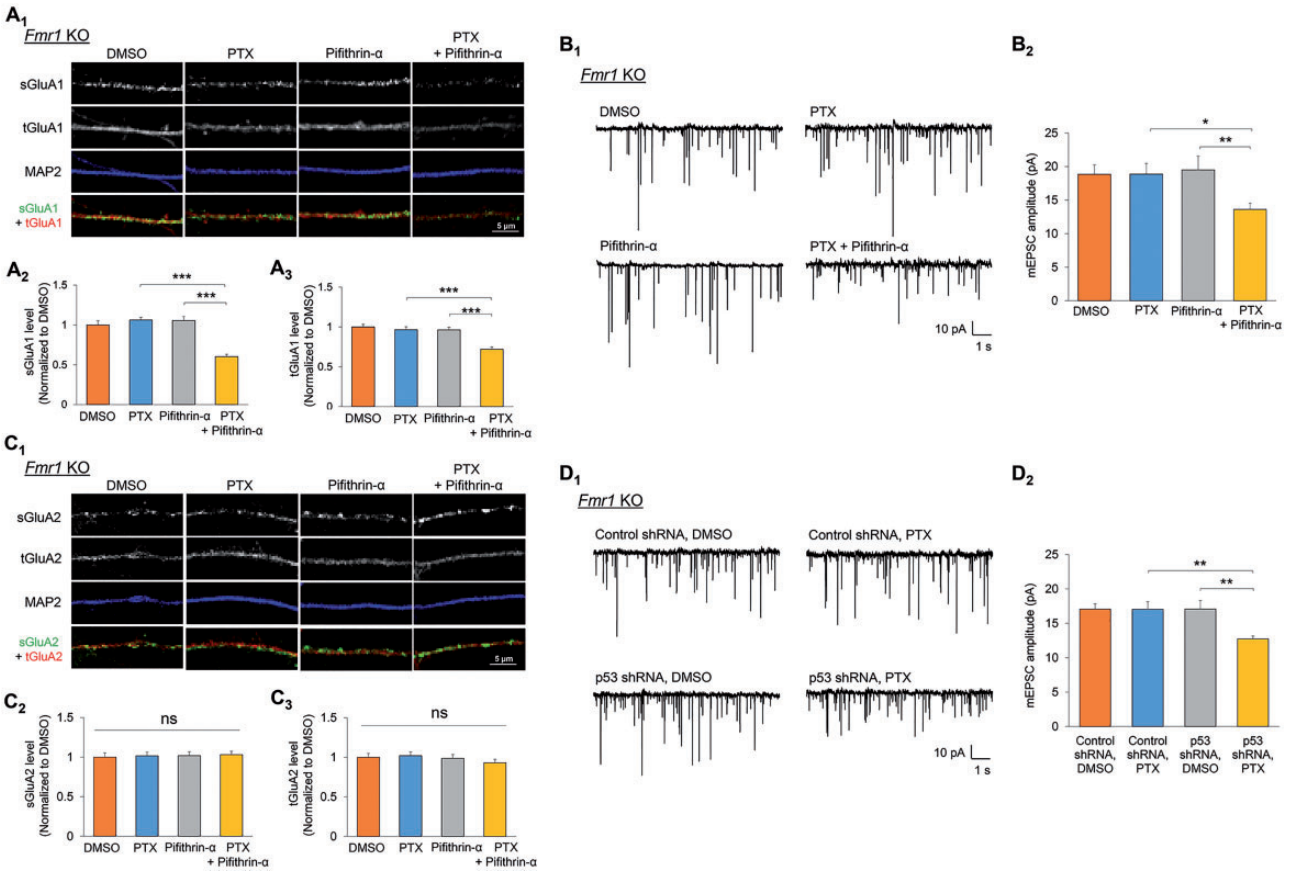

Figure 6. Inhibition of p53 restores homeostatic synaptic downscaling in *Fmr1* KO neurons. (**A**) Immunocytochemistry showing total (t) and surface (s) GluA1 in representative dendrites of *Fmr1* KO hippocampal neurons treated with vehicle (DMSO), PTX, pifithrin-α, or PTX + pifithrin-α for 48 h. Quantification of total and surface GluA1 normalized to the average intensity of that in DMSO-treated neurons are on the bottom ($n = 40$–41 cells). (**B**) Patch-clamp recording from *Fmr1* KO hippocampal neurons treated with DMSO, PTX, pifithrin-α or PTX + pifithrin-α for 48 h. Representative mEPSC traces and quantification of mEPSC amplitude are shown ($n = 19$–23 cells). (**C**) Immunocytochemistry showing total (t) and surface (s) GluA2 in representative dendrites of *Fmr1* KO hippocampal neurons treated with DMSO, PTX, pifithrin-α, or PTX + pifithrin-α for 48 h. Quantification of total and surface GluA2 normalized to the average intensity of that in DMSO-treated neurons are on the bottom ($n = 34$–37 cells). (**D**) Patch-clamp recording from *Fmr1* KO hippocampal neurons transfected with non-target shRNA (control shRNA) or p53 shRNA with DMSO or PTX for 48 h. Representative mEPSC traces and quantification of mEPSC amplitude are shown ($n = 20$–22 cells). Data were analyzed by two-way ANOVA with Tukey's test and represented as mean ± SEM with $^*P < 0.05$, $^{**}P < 0.01$, $^{***}P < 0.001$ and ns: non-significant.

Another scenario to explain abnormally stable p53 in *Fmr1* KO even when Mdm2 is hyperphosphorylated is that other molecules in *Fmr1* KO are interfering with the Mdm2-p53 interaction. The translation elongation factor 1-α (eEF1α), an Mdm2 interacting protein (33), is basally elevated owing to the loss of translational suppression in *Fmr1* KO (34,35). Our previous work showed that elevated Mdm2–eEF1α interaction in *Fmr1* KO alters the interactome of Mdm2 particularly in the nucleus (23). It is possible that eEF1α competes with p53 for binding to Mdm2 in *Fmr1* KO. If this is true, it would also explain how the lack of FMRP-dependent translation control contributes to the dysregulation of p53 down-regulation and homeostatic synaptic downscaling. We aim to test this possibility in a future study.

The functions of p53 in terminally differentiated neurons are largely unclear. Our current study demonstrated that down-regulation of p53 appears to be critical for maintaining Nedd4-2 phosphorylation and permitting synaptic downscaling. Furthermore, constitutive activity of p53 causes impaired synaptic downscaling in *Fmr1* KO neurons. Because synaptic scaling is crucial to brain circuit excitability homeostasis (1), this current study suggests p53 may be a novel molecule that could be targeted to alleviate neuronal hyperexcitability in FXS. Based on the deep knowledge of p53 that already exists in cancer biology and the many currently available drugs that target p53, further understanding of the roles of p53 may introduce new therapies into the study and treatment of FXS and other ASDs.

Materials and Methods

Animals and primary neuron cultures

WT and *Fmr1* KO mice in C57BL/6 background were obtained from The Jackson Laboratory. Primary hippocampal or cortical neuron cultures were made from mice, both male and female, at postnatal Day 0 (P0) or P1 as described previously (23). All experiments using animal data followed the guidelines of Animal Care and Use provided by the Illinois Institutional Animal Care and Use Committee (IACUC) and the guidelines of the Euthanasia of Animals provided by the American Veterinary Medical Association (AVMA) to minimize animal suffering and the number of animals used. This study was performed under an approved IACUC animal protocol of University of Illinois at Urbana-Champaign (#14139 and #17075 to N.-P.T.).

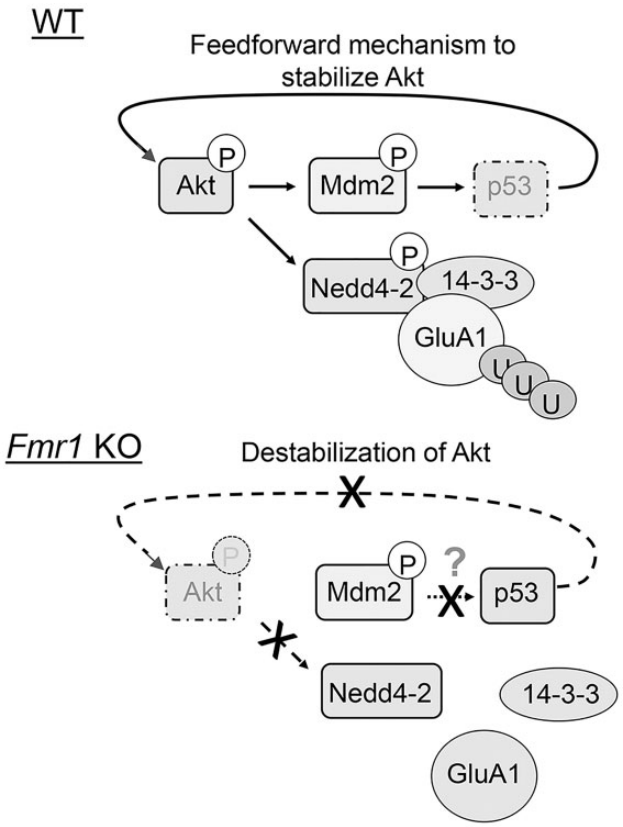

Figure 7. Working model of p53 and Nedd4-2 in FMRP-dependent homeostatic synaptic downscaling. In WT neurons, chronic activity stimulation triggers the Akt-Mdm2 pathway and leads to p53 down-regulation. A feedforward mechanism subsequently stabilizes Akt and promotes Nedd4-2 phosphorylation and the interaction between Nedd4-2 and 14-3-3. In *Fmr1* KO neurons, chronic activity stimulation fails to further elevate Mdm2 phosphorylation or trigger p53 down-regulation. Destabilized Akt leads to Nedd4-2 dephosphorylation and occludes GluA1 ubiquitination even in the presence of 14-3-3. Although Mdm2 is basally phosphorylated in *Fmr1* KO neurons, it is predicted that a compensatory mechanism is maintaining p53 level or an inhibitory molecule is interfering with Mdm2-p53 interaction in *Fmr1* KO neurons.

Reagents and constructs

DMSO was from Fisher Scientific. PTX was from Santa Cruz Biotechnology and pifithrin-α was from Adipogen Corporation. R18 was from Sigma-Aldrich. MG132 was from Selleck Chemical. Protein A/G beads and bovine serum albumins (BSA) were from Santa Cruz Biotechnology. Recombinant GluA1 and 14-3-3ϵ were from Origene. Recombinant Nedd4-2 was from Abnova. The antibodies used in this study were purchased from Santa Cruz Biotechnology (anti-p53 and anti-Mdm2), Cell Signaling (anti-*p*-Mdm2, anti-*p*-Akt, anti-Nedd4-2, anti-*p*-Nedd4-2, anti-pan-14-3-3 and anti-Ubiquitin), Millipore (anti-GluA1-N-terminus and anti-GluA2-N-terminus), Sigma-Aldrich (anti-GluA2-C-terminus), Abcam (anti-MAP2 and anti-GluA1-C-terminus), ThermoScientific (anti-HA) and GenScript Corporation (anti-Akt and anti-Gapdh). The Nedd4-2 expression constructs were from Applied Biological Materials.

Immunocytochemistry

To stain for surface AMPARs, neurons were fixed with fixation buffer [4% paraformaldehyde and 4% sucrose in phosphate buffered saline (PBS)] for 7 min and incubated with a primary antibody against the N-terminus of either GluA1 or GluA2 overnight at 4°C under a non-permeabilizing condition. After washing with PBS, the neurons were incubated with fluorescence-conjugated secondary antibodies for 2 h at room temperature. After washing and permeabilization with an additional incubation with 0.2% Triton X-100 in PBS for 10 min, an incubation with anti-MAP2 antibody and an antibody against the C-terminus of either GluA1 or GluA2 was performed overnight at 4°C. After washing with PBS, fluorescence-conjugated secondary antibodies were then incubated for 2 h at room temperature. After final washes with PBS, coverslips were mounted onto glass slides. Images were obtained using a Zeiss LSM 700 confocal microscope with 40× magnification and three different laser lines (488, 555 and 633 nm). Pinhole was set to 1 airy unit for all experiments. Confocal microscope settings were kept with the same laser and scanning configurations to allow for comparison across conditions. For image analysis, the background-subtracted mean fluorescence intensity in three dendritic regions of 50 μm was analyzed per cell using ImageJ software (National Institute of Health) (13). The background signal in the nearby area without any neurons was measured at least three different regions during analysis. Detailed information about the antibodies used for immunocytochemistry can be found in Supplementary Material, Table S2.

Transfection, IP and western blotting

For transient transfection, both HEK cells (ATCC; CRL-1573) and primary hippocampal neurons were transfected using Lipofectamine 3000 (Invitrogen). Specifically for neurons, cells were transfected at days *in vitro* (DIV) 11 (for electrophysiology experiments) or 13 (for immunocytochemistry) for 30–60 min followed by replacing the culture medium with conditioned medium to minimize toxicity produced by Lipofectamine. For lentiviral transfection in primary cortical neurons used for biochemical experiments, cells were incubated with lentivirus at DIV 9. Lentivirus was prepared according to the manufacturer's (Applied Biological Materials) instruction.

For IP, cell lysates were obtained by sonicating pelleted cells in a co-IP buffer (50 mM Tris, pH 7.4, 120 mM NaCl, 0.5% Nonidet P-40). Eighty micrograms of total protein or protein mixtures after *in vitro* ubiquitination was incubated 2 h at 4°C with 0.5 μg of primary antibodies. For experiments assessing ubiquitinated proteins, MG132 (10 μM) was added before cell harvesting and during antibody incubation to stabilize ubiquitinated protein. Protein A/G agarose beads were added for another hour followed by washing with co-IP buffer three times. For western blotting, after SDS-PAGE, the gel was transferred onto a polyvinylidene fluoride membrane. After blocking with 1% BSA in buffer (20 mM Tris pH 7.5, 150 mM NaCl, 0.1% Tween-20), the membrane was incubated with primary antibody overnight at 4°C, followed by three 10-min washings with the same buffer. The membrane was then incubated with a horseradish peroxidase-conjugated secondary antibody (from Santa Cruz Biotechnology) for 1 h at room temperature, followed by another three 10-min washings. Finally, the membrane was developed with an ECL Chemiluminescent Reagent and X-ray films (11). Detailed information about the antibodies used for IP and western blotting can be found in Supplementary Material, Table S2.

Signals from the proteins of interest were normalized to the house-keeping protein Gapdh. For the phospho-specific proteins, the phospho-specific signals were normalized to the signal from the protein of interest that was obtained

simultaneously from a separate membrane. To minimize inconsistency, the cell lysate from a specific treatment was prepared in a single mixture before loading into different wells or gels. If two or more gels were used for detecting different proteins from a single set of samples, all gels were run and transferred to the PVDF membranes together in a single buffer system and the western blotting was conducted simultaneously for all membranes.

In vitro ubiquitination

When obtaining Nedd4-2 from WT or *Fmr1* KO cultures, 250 μg of total protein lysates were subjected to IP with anti-Nedd4-2 antibody. Following IP, the protein beads were incubated with 0.1 M glycine–HCl at pH 3.0 for 15 min with frequent pipetting to dissociate Nedd4-2 from the antibody and the beads. After centrifugation at 1000*g* for 3 min to remove the beads, the supernatant was added with 1 M Tris–HCl at pH 8.5 to neutralize. The neutralized solution containing Nedd4-2 was immediately used to perform *in vitro* ubiquitination with HA-Ub (Boston Biochem). Ub activating enzyme (UBE1) (Boston Biochem), UbcH5b/UBE2D2 (Boston Biochem) and recombinant GluA1 (Origene) was used as substrate as described previously (12,36).

Electrophysiology

Whole-cell patch-clamp recordings were made at room temperature (23–25°C) in a submersion chamber continuously perfused with artificial cerebrospinal fluid (aCSF) containing (in mM): 119 NaCl, 2.5 KCl, 4 $CaCl_2$, 4 $MgCl_2$, 1 NaH_2PO_4, 26 $NaHCO_3$ and 11 D-glucose, saturated with 95% O_2/5% CO_2 (pH 7.4, 310 mOsm). aCSF was supplemented with 1 μM TTX and 100 μM PTX for mEPSC measurements to block action potential-dependent EPSCs and $GABA_A$ receptors, respectively. Whole cell recording pipettes (~4–6 MΩ) were filled with intracellular solution containing (in mM): 130 K-gluconate, 6 KCl, 3 NaCl, 10 HEPES, 0.2 EGTA, 4 Mg-ATP, 0.4 Na-GTP, 14 Tris–phosphocreatine, 2 QX-314 (pH 7.25, 285 mOsm). Neurons at DIV 14–17 were used for electrophysiological analyses. Membrane potential was clamped at −60 mV. Neurons were not included in analyses if the resting membrane potential was >–45 mV, access resistance was >30 MΩ, or if access resistance changed by >20%. All recordings were performed with Clampex 10.6 and Multiclamp 700B amplifier interfaced with Digidata 1440A data acquisition system (Molecular Devices). Recordings were filtered at 1 kHz and digitized at 10 kHz. mEPSCs were analyzed with Mini Analysis Program (Synaptosoft) with a 5-pA threshold level. Raw data of mEPSC amplitude and frequency in each experiment are included in Supplementary Material, Table S1.

Experimental design and statistical analysis

In all experiments, both male and female mice were used to prepare primary neuron cultures. At least 3 l, randomized four to six mice each, were used in each experiment. ANOVA with post hoc Tukey's honest significant differences (HSD) or Fisher's least significant differences (LSD) tests were used for multiple comparisons between treatments or genotypes. Student's *t*-test was used for mEPSC data, for imaging, and for western blotting results when two conditions were compared. Specific sample numbers, including the numbers of cells or repeats, are indicated in the figure legends. Differences are considered significant at the level of $P < 0.05$.

Supplementary Material

Supplementary Material is available at *HMG* online.

Conflict of Interest statement. None declared.

Funding

School of Molecular and Cellular Biology, University of Illinois at Urbana-Champaign, by Simons Foundation (SFARI #336605 to N.-P.T.); Brain and Behavior Research Foundation NARSAD Young Investigator Grant (to N.-P.T.); and National Institute of Health (R01NS105615 to N.-P.T.).

References

1. Frischknecht, R., Chang, K.J., Rasband, M.N. and Seidenbecher, C.I. (2014) Neural ECM molecules in axonal and synaptic homeostatic plasticity. *Prog. Brain Res.*, **214**, 81–100.
2. Rajman, M., Metge, F., Fiore, R., Khudayberdiev, S., Aksoy-Aksel, A., Bicker, S., Ruedell Reschke, C., Raoof, R., Brennan, G.P., Delanty, N. *et al.* (2017) A microRNA-129-5p/Rbfox crosstalk coordinates homeostatic downscaling of excitatory synapses. *EMBO J.*, **36**, 1770–1787.
3. Davis, G.W. (2013) Homeostatic signaling and the stabilization of neural function. *Neuron*, **80**, 718–728.
4. Wondolowski, J. and Dickman, D. (2013) Emerging links between homeostatic synaptic plasticity and neurological disease. *Front. Cell Neurosci.*, **7**, 223.
5. Gross, C., Yao, X., Pong, D.L., Jeromin, A. and Bassell, G.J. (2011) Fragile X mental retardation protein regulates protein expression and mRNA translation of the potassium channel Kv4.2. *J. Neurosci.*, **31**, 5693–5698.
6. Iacoangeli, A. and Tiedge, H. (2013) Translational control at the synapse: role of RNA regulators. *Trends Biochem. Sci.*, **38**, 47–55.
7. Repicky, S. and Broadie, K. (2009) Metabotropic glutamate receptor-mediated use-dependent down-regulation of synaptic excitability involves the fragile X mental retardation protein. *J. Neurophysiol.*, **101**, 672–687.
8. Turrigiano, G. (2012) Homeostatic synaptic plasticity: local and global mechanisms for stabilizing neuronal function. *Cold Spring Harb. Perspect. Biol.*, **4**, a005736.
9. Yang, B. and Kumar, S. (2010) Nedd4 and Nedd4-2: closely related ubiquitin-protein ligases with distinct physiological functions. *Cell Death Differ.*, **17**, 68–77.
10. Allen, A.S., Berkovic, S.F., Cossette, P., Delanty, N., Dlugos, D., Eichler, E.E., Epstein, M.P., Glauser, T., Goldstein, D.B., Han, Y. *et al.* (2013) De novo mutations in epileptic encephalopathies. *Nature*, **501**, 217–221.
11. Jewett, K.A., Zhu, J. and Tsai, N.P. (2015) The tumor suppressor p53 guides glua1 homeostasis through Nedd4-2 during chrnoic elevation of neuronal activity. *J. Neurochem.*, **135**, 226–233.
12. Zhu, J., Lee, K.Y., Jewett, K.A., Man, H.Y., Chung, H.J. and Tsai, N.P. (2017) Epilepsy-associated gene Nedd4-2 mediates neuronal activity and seizure susceptibility through AMPA receptors. *PLoS Genet.*, **13**, e1006634.
13. Tsai, N.P., Wilkerson, J.R., Guo, W., Maksimova, M.A., DeMartino, G.N., Cowan, C.W. and Huber, K.M. (2012) Multiple autism-linked genes mediate synapse elimination via proteasomal degradation of a synaptic scaffold PSD-95. *Cell*, **151**, 1581–1594.

14. Lin, A., Hou, Q., Jarzylo, L., Amato, S., Gilbert, J., Shang, F. and Man, H.Y. (2011) Nedd4-mediated AMPA receptor ubiquitination regulates receptor turnover and trafficking. *J. Neurochem.*, **119**, 27–39.
15. Schwarz, L.A., Hall, B.J. and Patrick, G.N. (2010) Activity-dependent ubiquitination of GluA1 mediates a distinct AMPA receptor endocytosis and sorting pathway. *J. Neurosci.*, **30**, 16718–16729.
16. Widagdo, J., Chai, Y.J., Ridder, M.C., Chau, Y.Q., Johnson, R.C., Sah, P., Huganir, R.L. and Anggono, V. (2015) Activity-dependent ubiquitination of GluA1 and GluA2 regulates AMPA receptor intracellular sorting and degradation. *Cell Rep.*, **10**, 783–795.
17. Gilbert, J., Shu, S., Yang, X., Lu, Y., Zhu, L.Q. and Man, H.Y. (2016) β-Amyloid triggers aberrant over-scaling of homeostatic synaptic plasticity. *Acta Neuropathol. Commun.* **4**, 131.
18. Gainey, M.A., Hurvitz-Wolff, J.R., Lambo, M.E. and Turrigiano, G.G. (2009) Synaptic scaling requires the GluR2 subunit of the AMPA receptor. *J. Neurosci.*, **29**, 6479–6489.
19. Soden, M.E. and Chen, L. (2010) Fragile X protein FMRP is required for homeostatic plasticity and regulation of synaptic strength by retinoic acid. *J. Neurosci.*, **30**, 16910–16921.
20. Chandran, S., Li, H., Dong, W., Krasinska, K., Adams, C., Alexandrova, L., Chien, A., Hallows, K.R. and Bhalla, V. (2011) Neural precursor cell-expressed developmentally down-regulated protein 4-2 (Nedd4-2) regulation by 14-3-3 protein binding at canonical serum and glucocorticoid kinase 1 (SGK1) phosphorylation sites. *J. Biol. Chem.*, **286**, 37830–37840.
21. Singh, P.K., Singh, S. and Ganesh, S. (2013) Activation of serum/glucocorticoid-induced kinase 1 (SGK1) underlies increased glycogen levels, mTOR activation, and autophagy defects in Lafora disease. *Mol. Biol. Cell*, **24**, 3776–3786.
22. Lee, I.H., Dinudom, A., Sanchez-Perez, A., Kumar, S. and Cook, D.I. (2007) Akt mediates the effect of insulin on epithelial sodium channels by inhibiting Nedd4-2. *J. Biol. Chem.*, **282**, 29866–29873.
23. Tsai, N.P., Wilkerson, J.R., Guo, W. and Huber, K.M. (2017) FMRP-dependent Mdm2 dephosphorylation is required for MEF2-induced synapse elimination. *Hum. Mol. Genet.*, **26**, 293–304.
24. Han, C.T., Schoene, N.W. and Lei, K.Y. (2009) Influence of zinc deficiency on Akt-Mdm2-p53 and Akt-p21 signaling axes in normal and malignant human prostate cells. *Am. J. Physiol. Cell Physiol.*, **297**, C1188–C1199.
25. Ogawara, Y., Kishishita, S., Obata, T., Isazawa, Y., Suzuki, T., Tanaka, K., Masuyama, N. and Gotoh, Y. (2002) Akt enhances Mdm2-mediated ubiquitination and degradation of p53. *J. Biol. Chem.*, **277**, 21843–21850.
26. Gottlieb, T.M., Leal, J.F., Seger, R., Taya, Y. and Oren, M. (2002) Cross-talk between Akt, p53 and Mdm2: possible implications for the regulation of apoptosis. *Oncogene*, **21**, 1299–1303.
27. Gainey, M.A., Tatavarty, V., Nahmani, M., Lin, H. and Turrigiano, G.G. (2015) Activity-dependent synaptic GRIP1 accumulation drives synaptic scaling up in response to action potential blockade. *Proc. Natl. Acad. Sci. USA*, **112**, E3590–E3599.
28. Gilbert, J., Shu, S., Yang, X., Lu, Y., Zhu, L.Q. and Man, H.Y. (2016) beta-Amyloid triggers aberrant over-scaling of homeostatic synaptic plasticity. *Acta Neuropathol. Commun.*, **4**, 131.
29. Imbrosci, B., Neitz, A. and Mittmann, T. (2014) Focal cortical lesions induce bidirectional changes in the excitability of fast spiking and non fast spiking cortical interneurons. *PLoS One*, **9**, e111105.
30. Sharma, A., Hoeffer, C.A., Takayasu, Y., Miyawaki, T., McBride, S.M., Klann, E. and Zukin, R.S. (2010) Dysregulation of mTOR signaling in fragile X syndrome. *J. Neurosci.*, **30**, 694–702.
31. Frankland, P.W., Wang, Y., Rosner, B., Shimizu, T., Balleine, B.W., Dykens, E.M., Ornitz, E.M. and Silva, A.J. (2004) Sensorimotor gating abnormalities in young males with fragile X syndrome and Fmr1-knockout mice. *Mol. Psychiatry*, **9**, 417–425.
32. Louros, S.R. and Osterweil, E.K. (2016) Perturbed proteostasis in autism spectrum disorders. *J. Neurochem.* **139**, 1081–1092.
33. Frum, R., Busby, S.A., Ramamoorthy, M., Deb, S., Shabanowitz, J., Hunt, D.F. and Deb, S.P. (2007) HDM2-binding partners: interaction with translation elongation factor EF1alpha. *J. Proteome Res.*, **6**, 1410–1417.
34. Sung, Y.J., Dolzhanskaya, N., Nolin, S.L., Brown, T., Currie, J.R. and Denman, R.B. (2003) The fragile X mental retardation protein FMRP binds elongation factor 1A mRNA and negatively regulates its translation *in vivo*. *J. Biol. Chem.*, **278**, 15669–15678.
35. Darnell, J.C., Van Driesche, S.J., Zhang, C., Hung, K.Y., Mele, A., Fraser, C.E., Stone, E.F., Chen, C., Fak, J.J., Chi, S.W. *et al.* (2011) FMRP stalls ribosomal translocation on mRNAs linked to synaptic function and autism. *Cell*, **146**, 247–261.
36. Woelk, T., Oldrini, B., Maspero, E., Confalonieri, S., Cavallaro, E., Di Fiore, P.P. and Polo, S. (2006) Molecular mechanisms of coupled monoubiquitination. *Nat. Cell Biol.*, **8**, 1246–1254.